

# AltiMaP: Altimetry Mapping Procedure for Hydrography Data

Menaka Revel<sup>1,†</sup>, Xudong Zhou<sup>1</sup>, Prakat Modi<sup>1,2</sup>, Jean-François Cretaux<sup>3</sup>, Stephane Calmant<sup>4</sup>, and Dai Yamazaki<sup>1</sup>

<sup>1</sup>Global Hydrological Prediction Center, Institute of Industrial Science, The University of Tokyo, Tokyo, Japan.

5 <sup>2</sup>Department of Civil Engineering, Shibaura Institute of Technology, Tokyo, Japan.

<sup>3</sup>Laboratoire d'Études en Géophysique et Océanographie Spatiales (LEGOS), Centre National d'Études Spatiales (CNES) Toulouse, France.

<sup>4</sup>Institute of Research for Development, France.

10 <sup>†</sup>Now at Department of Civil and Environmental Engineering, University of Waterloo, Canada.

*Correspondence to:* Menaka Revel (menaka@rainbow.iis.u-tokyo.ac.jp)

## Abstract

Satellite altimetry data are useful for monitoring water surface dynamics, evaluating and calibrating hydrodynamic models, and enhancing river-related variables through optimization or assimilation approaches. However, comparing simulated water surface elevations (WSEs) using satellite altimetry data is challenging due to the difficulty of correctly matching the representative locations of satellite altimetry virtual stations (VSs) to the discrete river grids used in hydrodynamic models. In this study, we introduce an automated altimetry mapping procedure (AltiMaP) that allocates VS locations listed in the HydroWeb database to the Multi-Error Removed Improved Terrain Hydrography (MERIT Hydro) river network. Each VS was flagged according to the land cover of the initial pixel allocation, with 10, 20, 30, and 40 representing river channel, land with the nearest single-channel river, land with the nearest multi-channel river, and ocean pixels, respectively. Then, each VS was assigned to the nearest MERIT Hydro river reach according to geometric distance. Among the approximately 12,000 allocated VSs, most were categorized as flag 10 (71.7%). Flags 10 and 20 were mainly located in upstream and midstream reaches, whereas flags 30 and 40 were mainly located downstream. Approximately 0.8% of VSs showed bias, with considerable elevation differences ( $\geq |15|m$ ) between the mean observed WSE and MERIT digital elevation model. These biased VSs were predominantly observed in narrow rivers at high altitudes. Following VS allocation using AltiMaP, the median root mean squared error of simulated WSEs compared to satellite altimetry was 7.86 m. The error rate was improved meaningfully (10.6%) than that obtained using a traditional approach, partly due to bias reduction. Thus, allocating VSs to a river network using the proposed AltiMaP framework improved our comparison of WSEs simulated by the global hydrodynamic model to those obtained by satellite altimetry. The AltiMaP source code (<https://doi.org/10.5281/zenodo.7597310>) (Revel et al., 2023a) and data (<https://doi.org/10.4211/hs.632e550deaca46b080bdae986fd19156>) (Revel et al., 2022) are freely accessible online and we anticipate that they will be beneficial to the international hydrological community.

## 35 1 Introduction

Limited freshwater resources could impede the daily demands of future generations. Monitoring freshwater resources is critical for determining the availability of water for human use. Although continental surface water dynamics can be explored through global-scale hydrodynamic modeling, the effective modeling of freshwater dynamics requires calibration using observed variables such as water surface elevation (WSE), river discharge, and water surface area. Thus, inadequacies of monitoring stream gauges can hinder the performance of hydrodynamic models and fail to accurately represent surface water dynamics (Hannah et al., 2011), such that model evaluation and calibration must depend on remotely sensed data (Meyer Oliveira et al., 2021; Modi et al., 2022; Zhou et al., 2022). Therefore, recent advances in satellite technology have considerably improved our understanding of surface water dynamics.

Satellite altimetry has facilitated direct and reasonably accurate measurements of terrestrial water levels over the past 30 years, with uncertainties ranging from a few centimeters to a few decimeters depending on the environment and altimeter employed. (Cretaux, 2022; Papa et al., 2022). Satellite altimeters determine WSEs by considering differences in the travel time of radar or lasers between the satellite and the water surface. Differences between satellite orbit and altimetry range measurements are used to determine the height of the water surface following dry troposphere, wet troposphere, ionospheric, and/or solid tide correction (Calmant et al., 2008). Several radar altimetry missions have been employed to observe lakes and large rivers, including Topography Experiment (TOPEX)/Poseidon; European Remote Sensing (ERS)-1 and -2; Joint Altimetry Satellite Oceanography Network (Jason)-1, -2, and -3; GEOSTAT Follow On (GFO); Environmental Satellite (ENVISAT); Satellite with ARGOS and ALTIKA (SARAL)-A1tiKa; Sentinel-3A, -3B, and -6MF (Calmant et al., 2008; Crétaux et al., 2009, 2011; Santos da Silva et al., 2010; Yang et al., 2022). An updated list of orbit characteristics including temporal resolution, inter-track distance, and frequency for satellite missions that have collected WSE observations is provided in Table 1. In particular, satellite temporal resolution and inter-track distance govern the temporal and spatial resolution of altimetry data. Higher temporal resolution, achieved through frequent passes or shorter revisit times, captures temporal changes with finer granularity, while a smaller inter-track distance provides a higher spatial resolution by offering closely spaced measurements. Consequently, a combination of higher temporal and spatial resolutions in satellite altimetry data enhances the ability to monitor the dynamic processes in the terrestrial surface waters.

Any intersection of a satellite track with a water body is considered a virtual station (VS). The allocation of VSs permits a satellite to retrieve successive water levels at each pass (Santos da Silva et al., 2010). The river width and shape, surrounding topography, and land cover are important factors influencing successful water level retrievals, although no single factor is solely predictive of water level accuracy (Maillard et al., 2015). As a result, radar altimetry retrievals of river surface height depend on the high dielectric constant of water, which causes rivers to reflect more radar radiation than land. It is also challenging to identify exact VS locations due to satellite orbit drift. Therefore, the location of a VS is frequently recorded as the center point of the search area for water level retrieval (Coss et al., 2020; Santos da Silva et al., 2010). To facilitate comparative analyses between satellite observations and numerical simulations, caution must be exercised when transforming the latitude and longitude coordinates of VSs to the river network of the hydrodynamic model.

Satellite altimetry observations have been applied in several large-scale studies to monitor natural water resources in rivers and lakes (e.g., Asadzadeh Jarihani et al., 2013; Birkett et al., 2002; Calmant and Seyler, 2006; Dettmering et al., 2020; Schneider et al., 2017; Xiang et al., 2021), calibrate or validate hydrological/hydrodynamic models (e.g., Elmer et al., 2021; Jiang et al., 2019, 2021; Kittel et al., 2021; Meyer Oliveira et al., 2021; Zhou et al., 2022), and for assimilation into hydrological/hydrodynamic models (e.g., Brêda et al., 2019; Michailovsky et al., 2013; Paiva et al., 2013; Revel et al., 2023b). However, incorrect VS allocation can lead to the degradation of post-calibration model performance. Thus, the accurate identification of appropriate VS locations within the relevant river reach in the model space is crucial for the comparison of simulation and observation data, as well as for the effective utilization of satellite altimetry in model calibration and validation.

Large-scale hydrodynamic models typically simulate the water dynamics of discretized river segments (i.e., river grids). The slopes of natural rivers are continuous, whereas elevations are discontinuous among river grids; thus, the digitized VSs can be located between river grids. Physically based hydrodynamic models simulate WSEs with respect to a representative elevation within the river grid which were upscaled from high-resolution hydrography data (i.e., the lowest elevation of high-resolution pixels within the river grid) (Yamazaki et al., 2009, 2011). As a result, the ground elevation of the simulation and observation location can be different, leading to elevation bias between simulated and observed WSEs. Furthermore, river networks are typically delineated using digital elevation models (DEMs), which suffer from inherent errors (Hawker et al., 2019, 2022; Yamazaki et al., 2017). Therefore, river networks used in large-scale models may contain deviations from the courses of actual rivers (Amatulli et al., 2022; Paz et al., 2006; Yamazaki et al., 2009). To understand the ability of large-scale hydrodynamic models to represent actual WSEs, which is critical for comparing and validating the simulated WSE, an understanding relative location of VS within the river grid is needed.

Apart from other model limitations such as uncertainty in model parameters, simplified physics, and bias in forcing, the discrepancy in the virtual station location in the river network is a considerable contributor to the bias in simulated water surface elevation when compared to satellite altimetry observations. Large-scale model calibration studies have utilized WSE anomalies for comparison with simulations, where the rough allocation of VSs in the river proves suitable (e.g., Meyer Oliveira et al., 2021; De Paiva et al., 2013). Conversely, small-scale studies have manually allocated VSs along the river centerline (e.g., Domeneghetti et al., 2021; Jiang et al., 2019, 2021a; Schneider et al., 2017). Calibrations requiring absolute WSE observations, such as calibration of river bottom elevation using rating curves, demand meticulous allocation of virtual stations (VSs) within the river pixels (Zhou et al., 2022). To effectively utilize satellite altimetry observations for supporting large-scale hydrodynamic model development, a method is required to map representative locations of VSs to relevant river pixels. Moreover, an automated mapping approach becomes essential to facilitate the global-scale model evaluations. Therefore, the development of an automated method for mapping VSs into the river network is paramount to the evaluation of hydrodynamic models on a global scale. We introduce our automated altimetry mapping procedure (AltiMaP), which enable better evaluation of WSEs simulated by large-scale hydrodynamic models using available satellite altimetry data. AltiMaP reduces the incidence of mismatches between VS locations and actual river locations, which are caused by DEM errors, the use of discrete river grids, and the allocation of VSs to the center of the WSE observation search area. We used pre-processed satellite altimetry data obtained from HydroWeb (<https://hydroweb.theia-land.fr>, last access: 2 February 2023) to assign VS locations to the high-resolution DEM-

based Multi-Error Removed Improved Terrain Hydrography (MERIT Hydro) flow direction map (Yamazaki et al., 2019). Simulations were conducted using the Catchment-based Macro-scale Floodplain (CaMa-Flood) global river hydrodynamic model (Yamazaki et al., 2011) which uses an upscaled river network of MERIT Hydro flow direction map using Flexible Location of Waterways (FLOW: Yamazaki et al., 2009) algorithm, to evaluate VS allocation accuracy by comparing satellite altimetry WSE observations with simulation results using AltiMaP and a traditional VS allocation method.

**Table 1: Satellites altimetry missions which are commonly used for water surface elevation observations. Some characteristics are outlined such as nominal orbit period, temporal resolution, intertrack difference, orbit height, inclination, retracker, agency and data source.**

Satellite	Norminal Orbit Period	Temporal Resolution (days)	Inter-track distacne at Equater (km)	Orbit Height (km)	Inclination (°)	Retracker	Agency	Data Source
T/P	1992-2006	10	315	1336	66	onboard	NASA - CNES	PODAAC
ERS-1	1991-2000	35	80	785	98.52	ICE-1, ICE-2	ESA	ESA
ERS-2	1995-2011	35	80	785	98.52	ICE-1, ICE-2	ESA	ESA
GFO	1998-2008	17	165	784	108	Ocean	US Navy / NOAA	NOAA
ENVISAT	2002-2012	35	80	800	98.55	ICE-1	ESA	ESA
Jason-1	2001-2013	10	315	1336	66	ICE	NASA - CNES	AVISO
Jason-2	2008-2016*	10	315	1336	66	ICE-3	NASA - CNES - EUMESTA T - NOAA	AVISO
Jason-3	2016-2022*	10	315	1336	66	ICE	NASA - CNES - EUMESTA T - NOAA	AVISO
SARAL/Alt iKa	2013-2016*	35	75	800	98.5	ICE-1	ISRO - CNES	AVISO
Sentinel-3A	2016-Current	27	104	814.5	98.65	OCOG	ESA	COPERNI CUS
Sentinel-3B	2018-Current	27	52	814.5	98.65	OCOG	ESA	COPERNI CUS
Sentinel-6MF	2022-Current	10	315	1336	66	OCOG	ESA	COPERNI CUS

## 2 Data and Methods

Satellite altimetry data are increasingly used in observing surface water dynamics as their availability has improved. However, it is essential to develop a framework to deploy altimetry data in the calibration and validation of surface water dynamics simulations. The AltiMaP algorithm was developed for use with the MERIT Hydro flow direction map, although it can be applied to other flow direction maps using the “deterministic eight neighbors” (D8) form, in which the downstream direction is determined by one of the eight neighboring pixels. The CaMa-Flood model discretizes river networks in terms of irregular-shaped unit-catchments and uses the elevation of the unit catchment river mouth (i.e., the lowest elevation of the unit catchment) as the riverbank elevation for that river segment. Therefore, to compare observed WSEs with those simulated by a large-scale

hydrodynamic model such as CaMa-Flood, one can allocate VS location to the MERIT Hydro flow direction map and map it into a coarser-resolution river network.

The accurate allocation of each VS to the MERIT Hydro by AltiMaP involves three main steps: conversion of the VS longitude and latitude to the x- and y-coordinates of a 3" pixel (~90 m × 90 m at the equator), flagging the VS according to the land cover of the pixel, and allocation of the flagged VS to the nearest river channel on the MERIT Hydro flow direction map. This study introduces the concepts and an overview of the satellite altimetry allocation algorithm; the source code (<https://doi.org/10.5281/zenodo.7597310>, Revel et al., 2023a) and dataset prepared for HydroWeb using AltiMaP for use with MERIT Hydro (<https://doi.org/10.4211/hs.632e550deaca46b080bdac986fd19156>, Revel et al., 2022) are provided.

## 140 **2.1 Satellite altimetry data**

Satellite altimetry observes water surface heights by measuring the time it takes for radar/laser pulses to bounce back from smooth surfaces. Although satellite altimetry missions were developed for ocean surface observations, they have increasingly been applied to observe lakes and rivers (Abdalla et al., 2021; Calmant et al., 2008; Calmant and Seyler, 2006; Yang et al., 2022). Several agencies have already processed their original satellite altimetry data and produced data archives for studying WSEs, including the HydroWeb (Créaux et al., 2011; Santos da Silva et al., 2010), Hydrosat (Tourian et al., 2016, 2022), Database for Hydrological Time Series of Inland Waters (DAHITTI; Schwatke et al., 2015), Global Reservoirs and Lakes Monitor (G-REALM; Birkett and Beckley, 2010), Copernicus Global Land Service (CGLS; Calmant et al., 2013; Créaux et al., 2011), River & Lake (Birkett et al., 2002), Hidrosat (Santos da Silva et al., 2010; da Silva et al., 2012), and Global River Radar Altimetry Time Series (GRRATS; Coss et al., 2020) archives. In this study, we utilized satellite altimetry data obtained from HydroWeb (<https://hydroweb.theia-land.fr>, last accessed on 2 February 2023), which offered 12523 VSs at the time of data acquisition. For the study, we considered all available VSs from HydroWeb due to its convenient data retrieval process and global coverage. Initially, we identified all the VSs listed in HydroWeb as potential candidates for inclusion in this research.

## 155 **2.2 Hydrography data**

An accurate flow direction map is essential for simulating realistic surface water dynamics at the global scale. The river network used in this study is a 3" flow direction map derived from the MERIT DEM (Yamazaki et al., 2017) and water body datasets including the Global 1" Water Body Map (G1WBM; Yamazaki et al., 2015), Global Surface Water Occurrence (GSWO; Pekel et al., 2016), and OpenStreetMap, which are referred to as MERIT Hydro (Yamazaki et al., 2019). The MERIT Hydro generation involved following steps. Initially a "conditioned DEM" was created by lowering the elevation of water pixels in MERIT DEM based on G1WBM, GSWO, and OpenStreetMap. Subsequently, an initial flow direction was determined based on topographic slope using "Steepest Slope Method". Some adjustments were made to ensure the flow continuity. Finally, endorheic basins were detected using Global 3" Water Body Map and Landsat tree density maps (Yamazaki et al., 2019). The MERIT Hydro include an adjusted DEM, river width, height over the nearest drainage, flow accumulation area,

and flow direction data. The 3" MERIT Hydro was used to determine whether VSs were located on land, river, or ocean pixels. The allocation procedure for the higher-resolution flow direction map is described in Section 2.3.

### 2.3 Allocation of VSs to the MERIT Hydro

VSs must be assigned to river network pixels of the hydrodynamic model for accurate comparison of simulated and observed WSEs. The DEM-based river network can deviate from the cause of the actual river due to errors in DEM and low representability of the coarse-resolution of the river network (Amatulli et al., 2022; Paz et al., 2006; Yamazaki et al., 2009). Moreover, the reported location of the VS provided in HydroWeb can be further away from the actual river because HydroWeb provides the center of the search region, within a range of a few kilometers (e.g., 5 km × 5 km). Therefore, an important step in allocating VSs to large-scale hydrodynamic models is to assign each VS to a river centerline on a higher-resolution flow direction map (e.g., MERIT Hydro, at 3"). A schematic diagram of this allocation process is shown in Figure 1. Initially, the satellite altimetry auxiliary data (e.g., longitude and latitude) for each VS were converted into 3" pixels. Then we flagged each VS according to the land cover of the initial allocation of the pixel, with 10, 20, 30, and 40 representing river channel, land with the nearest single-channel river, land with the nearest multi-channel river, and ocean pixels, respectively (Figure 1). The secondary flags also defined to represents more special cases as defined supplementary Table S1. Finally, we searched for the centerline of the nearest river according to geometric distance and allocated the VS to that location. VSs initially located on land pixels with the nearest multi-channel rivers were allocated to the nearest largest channel of the multi-channel river (considering the upstream catchment area). The AltiMaP identifies multi-channel river by searching in a direction perpendicular to the specified river considering their downstream connectivity. We assume the observation is from the largest river when there are multiple river (Supplementary

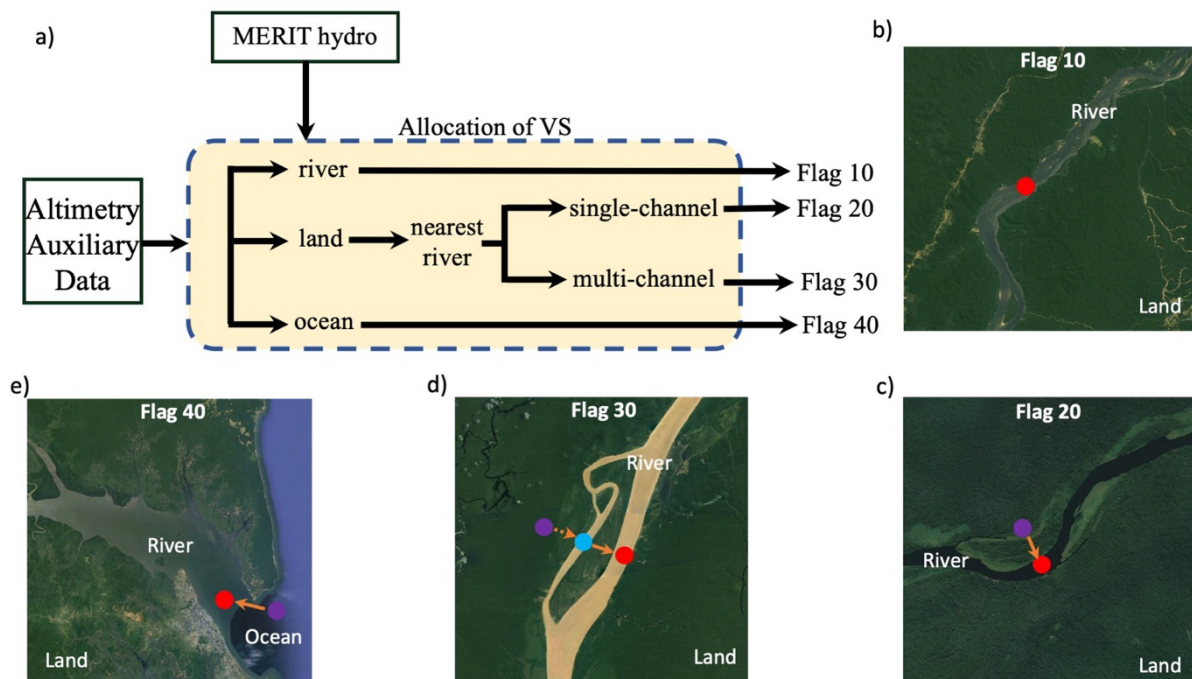


**Figure 1: Schematic diagram of allocating virtual stations (VS) to MERIT-hydro river network. The panels b, c, d, and e present schematics corresponding to Flag 10, Flag 20, Flag 30, and Flag 40, respectively. Red, blue, and purple dots are for final, secondary, and initial locations of VS allocation. (© Google Earth 2022)**

Figure S1) channels near the VS location because backscatter from the narrow river can be highly influenced by non-water features and mostly successful retrievals of WSE can be seen on larger rivers than  $\sim 0.8$  km. (Birkett et al., 2002).

## 2.4 Filtering biased stations

190 Even when VSs were aligned perfectly with the river network, simulated WSEs obtained using the river network deviated from satellite altimetry observations. These deviations were caused by errors in the parameters (e.g., riverbank height or river bathymetry [Supplementary Text S1]) and/or the forcings (e.g., surface and subsurface runoff), although satellite altimetry for inland waters can also contain errors (Biancamaria et al., 2017; Frappart et al., 2006; Santos da Silva et al., 2010). The satellite altimetry data should be within a relatively comparable  
 195 limit with simulated WSE to calibrate or validate the large-scale hydrodynamic models. Since the ground elevations were not recorded at the VS, we compared the mean of the satellite altimetry WSE at the VS with MERIT DEM elevation corresponding to the allocated locations of that particular VSs in the MERIT Hydro flow direction map at 3"-resolution. Then we removed VSs with mean WSEs that were  $\geq 15$  m higher or lower than the MERIT DEM elevation of the corresponding pixel. These limits were selected in consideration of variation in  
 200 the flow (Coss et al., 2020) and flood wave height of large rivers (Trigg et al., 2009). We determined that these constraints would be sufficient to include any river surface measurements within a comparable limit, given the elevation data used in this study; however, this threshold can be changed readily to meet user requirements. An example of the application of these restraints for a main Congo channel is provided in Figure 2, in which an unreasonably high VS allocation was removed as biased.

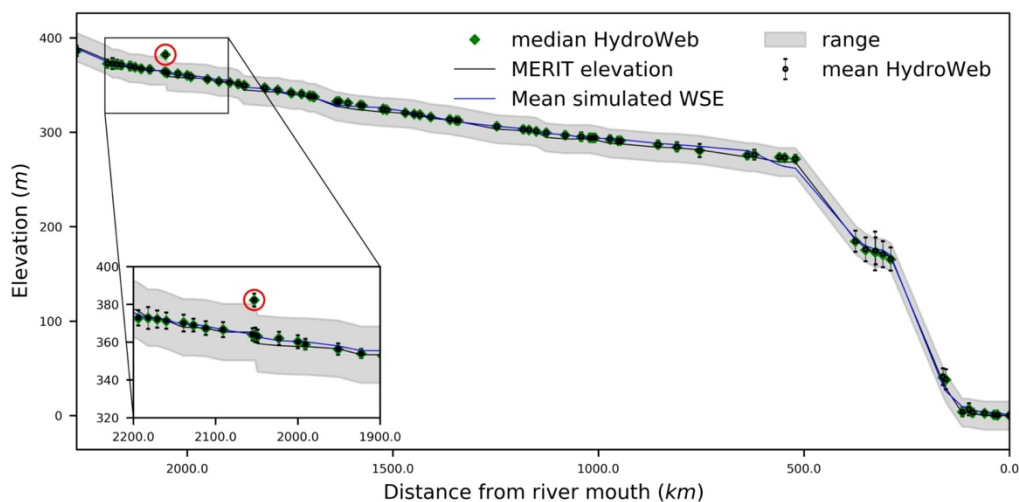


**Figure 2: Example of virtual station (VS) showing unrealistic observations in Congo mainstream. MERIT riverbank elevation; upper and lower limit; and mean simulated WSE using CaMa-Flood hydrodynamic model with VIC BC runoff is shown in grey lines, grey shades, and blue lines, respectively. Black dots and green diamonds indicates the mean and median satellite altimetry height. The standard deviation is shown in black error bars.**

205 **2.5 Comparison with simulated WSEs**

We used the CaMa-Flood v4.0 model (Yamazaki *et al.*, 2011), which has a spatial resolution of 6' to evaluate the performance of the AltiMaP VS allocation method. CaMa-Flood determines river hydrodynamics using a local inertial flow equation (Bates *et al.*, 2010; Yamazaki *et al.*, 2011). The model is forced by runoff (surface and subsurface water flow per unit area) from a land surface model (LSM) to route the water through a river. CaMa-Flood is a physical model that simulates floodplain dynamics and complex hydrodynamics including the hysteresis (Yamazaki *et al.*, 2011, 2012), and flow bifurcation (Yamazaki *et al.*, 2014b). Incorporating accurate DEMs such as MERIT DEM (Yamazaki *et al.*, 2017, 2019) into the CaMa-Flood has enabled it to represent WSE dynamics more accurately compared to satellite altimetry (Modi *et al.*, 2022). Because CaMa-Flood uses the lowest elevation of the unit-catchment as the elevation of the river segment, and VSs are located where the satellite track crosses the river, which may occur elsewhere within the unit catchment, there may be elevation differences between observed and simulated WSEs (Figure 3). Therefore, evaluating elevation differences between VS locations and unit catchment outlets is important.

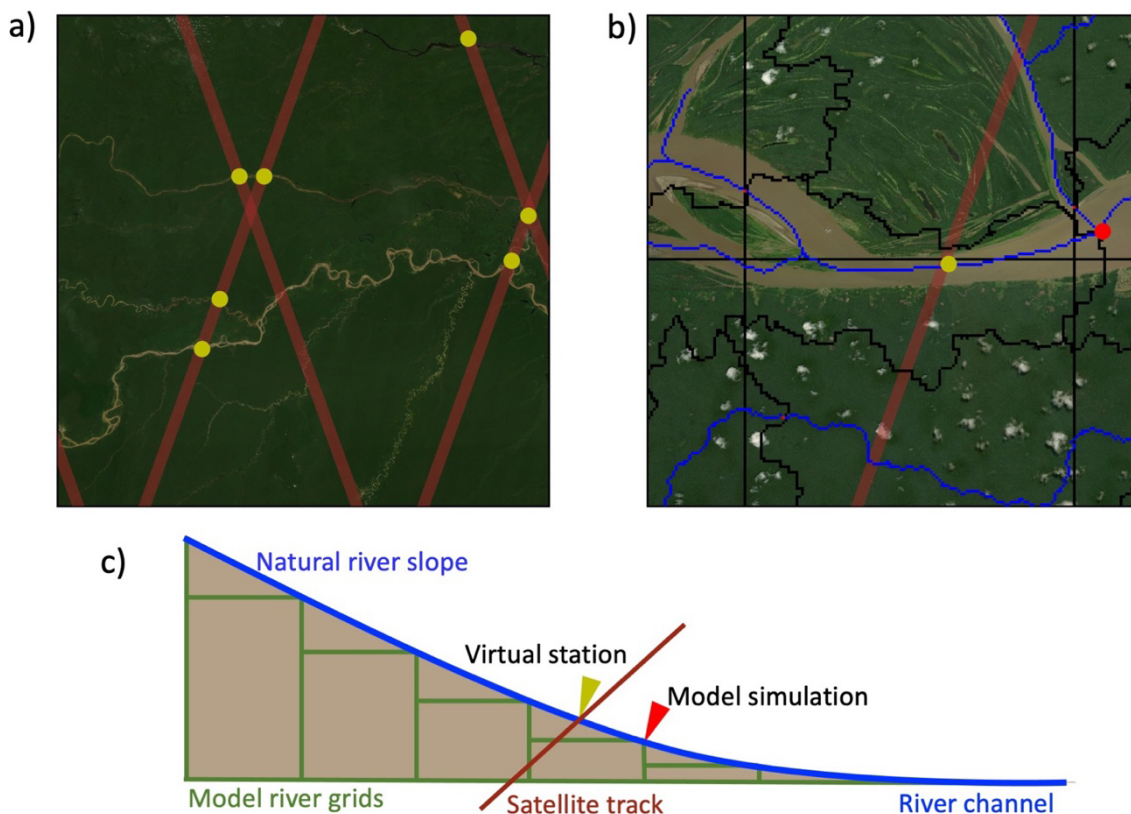


**Figure 3: Representation of Virtual Station (VS) in the river network map for large-scale hydrodynamic model. a) Satellite tracks, b) VS representation in unit-catchment, and c) longitudinal section of the river. Yellow and red color points indicate the VS locations and unit-catchment mouth. The model simulation is corresponding to the unit-catchment mouth corresponding to red point. (Aerials are from Esri, DigitalGlobe, GeoEye, i-cubed, USDA FSA, USGS, AEX, Getmapping, Aerogrid, IGN, IGP, swisstopo, and the GIS User Community)**



We forced the CaMa-Flood hydrodynamic model using the runoff simulated by the Variable Infiltration Capacity (VIC) LSM (Liang et al., 1994) with bias correction (VIC BC) (Lin et al., 2019). The standard model parameters were used in this simulation including parameters such as river bathymetry, river width, and Manning’s coefficient. For comparison with WSEs simulated by CaMa-Flood, we mapped VSs to a 6’-resolution global river network after allocating VSs to the MERIT Hydro network at 3’’-resolution using AltiMaP, because the CaMa-Flood river map was derived by upscaling the MERIT Hydro flow direction map using FLOW algorithm (Yamazaki et al., 2009). Then we compared the resulting simulated WSEs with observed WSEs mapped onto the river network based on the MERIT Hydro using the AltiMaP algorithm and the ordinary allocation method, i.e., converting longitude and latitude to the CaMa-Flood grid. In this evaluation, our primary objective is to assess the potential improvement brought about by the AltiMaP method when comparing simulated WSE with the ordinary allocation method. For a fair and unbiased evaluation, we employ the same dataset for both observations (i.e., satellite altimetry) and simulations. By doing so, we create a consistent and controlled environment to assess the performance of the AltiMaP method in comparison to the ordinary allocation method. We would like to emphasize that our intention is not to treat the CaMa-Flood simulation results as an absolute reference. Rather, we utilize them as a basis for evaluating the allocation methods concerning satellite altimetry data. Our aim is to investigate whether the AltiMaP method offers any notable advancements in the accuracy of simulated WSEs when compared to satellite-derived measurements.

## 2.6 AltiMaP variable identification

The AltiMaP variables provided for each VS are listed in Table 2; the full dataset is provided in <https://doi.org/10.4211/hs.632e550deaea46b080bdae986fd19156> (Revel et al., 2022). The data primarily includes variables related to VS metadata, VS allocation to the MERIT Hydro, and VS mapping to a coarse-resolution river network (e.g., global 6’). The VS metadata consists of the VS ID, name, longitude, latitude, and satellite name. Important parameters for VS allocation that are related to the MERIT Hydro river network can also be calculated for other river network datasets, by flagging and allocating VSs as described in Section 2.3, and then adding 100 to the flag of any VS that is biased (Section 2.4). The distance from a VS mapped to a river centerline to the unit catchment river mouth is an important parameter for understanding differences in water surface dynamics between simulated and satellite altimetry observations. The best and second-best candidate locations for VSs on the MERIT Hydro river centerline ( $10^\circ \times 10^\circ$  grid) are also reported, along with their geometric distances from the VS location; for single-channel rivers, these data are not available. The river width at each VS location mapped onto the MERIT Hydro river network was calculated using satellite-based water masks and flow direction maps (Yamazaki et al., 2014a). The distance from the VS to the best and second option locations on MERIT Hydro is also included. The coarse-resolution river network variables include the x and y coordinates for the global 6’ map used in the large-scale hydrodynamic model, as well as the elevations of the Earth Gravitational Model 2008 (EGM08) and Earth Gravitational Model 1996 (EGM96).

**Table 2: AltiMaP data description. The data can be divided into three basic categories namely, VS metadata, MERIT Hydro-related, and coarser-resolution river network-related.**

Variable	Description	Units
----------	-------------	-------

VS metadata		
ID	Identification number of VS	-
station	VS name	-
dataname	dataset name	-
lon	longitude	degrees east
lat	latitude	degrees north
satellite	name of the satellite	-
MERIT Hydro-related		
flag	allocation flag	-
elevation	elevation at VS location on MERIT Hydro	m
dist_to_mouth	distance to the unit-catchment mouth	km
kx1	best x-coordinate with respect to the $10^\circ \times 10^\circ$ higher resolution tile	-
ky1	best y-coordinate with respect to the $10^\circ \times 10^\circ$ higher resolution tile	-
kx2	second-best option of x-coordinate with respect to the $10^\circ \times 10^\circ$ high-resolution tile	-
ky2	second-best option of y-coordinate with respect to the $10^\circ \times 10^\circ$ high-resolution tile	-
dist1	distance from the second-best location to the VS	km
dist2	distance from the second-best location to the VS	km
rivwth	River width of the allocated location	m
Coarse-resolution river network-related		
ix	x-coordinate with respect to coarse resolution	-
iy	y-coordinate with respect to coarse resolution	-
EGM08	EGM 2008 datum elevation	m
EGM96	EGM 1996 datum elevation	m

### 3 Results

255 The AltiMaP dataset produced allocation locations for 12,523 VSs worldwide that are listed in the HydroWeb database. In this section, we discuss the characteristics of VS flags and conditions that can lead to considerable bias in satellite altimetry compared to the MERIT DEM.

### 3.1 Allocation of VSs to the river network

Figure 4a shows the global distribution of flags 10, 20, 30, and 40, which VSs initially located on river channel, land with a single-channel river nearby, land with a multi-channel river nearby, and ocean pixels, respectively. Flag 10 was the most common, accounting for 71.74% of all VSs, followed by flags 20 (26.88%), 30 (1.34%), and 40 (0.04%). Flags 10 and 20 were evenly distributed worldwide. Mostly, large rivers such as Amazon, Congo, Nile, Ob, etc. consist of flags 10 or 20 which indicate the low inconsistencies between VS locations and the river network. Flag 40 is distributed near the ocean in Congo River, Santee River in United States, Lumi Semanit River in Albania, Mahavavy River in Madagascar, and Luni River in India. In addition, flag 30 can be seen mostly in mid-streams where multi-channel rivers exist. Hence, different flags shows different geographical characteristics.

The log probability distributions of upstream catchment areas for different flag values are also shown in Figure 4b. The median upstream catchment areas were  $2.73 \times 10^4$ ,  $9.95 \times 10^3$ ,  $2.16 \times 10^4$ , and  $3.95 \times 10^4$  km<sup>2</sup> for flags 10, 20, 30, and 40, respectively. Flag 40 represented the largest median upstream catchment area because those are closer to the ocean and have large upstream catchment area. The distribution of flag 40 was strongly right skewed, influenced by the larger upstream catchment area of downstream Congo River. Flag 20 had the smallest median upstream catchment area, which indicates that most flag 20 VSs were in upstream reaches.

Figure 4c depicts the probability distribution of riverbank elevation for each flag. Lines represent the probability distributions of elevation for flags 10 to 30, with median values of 112.9m, 147.0m, and 141.2m for flag 10, flag

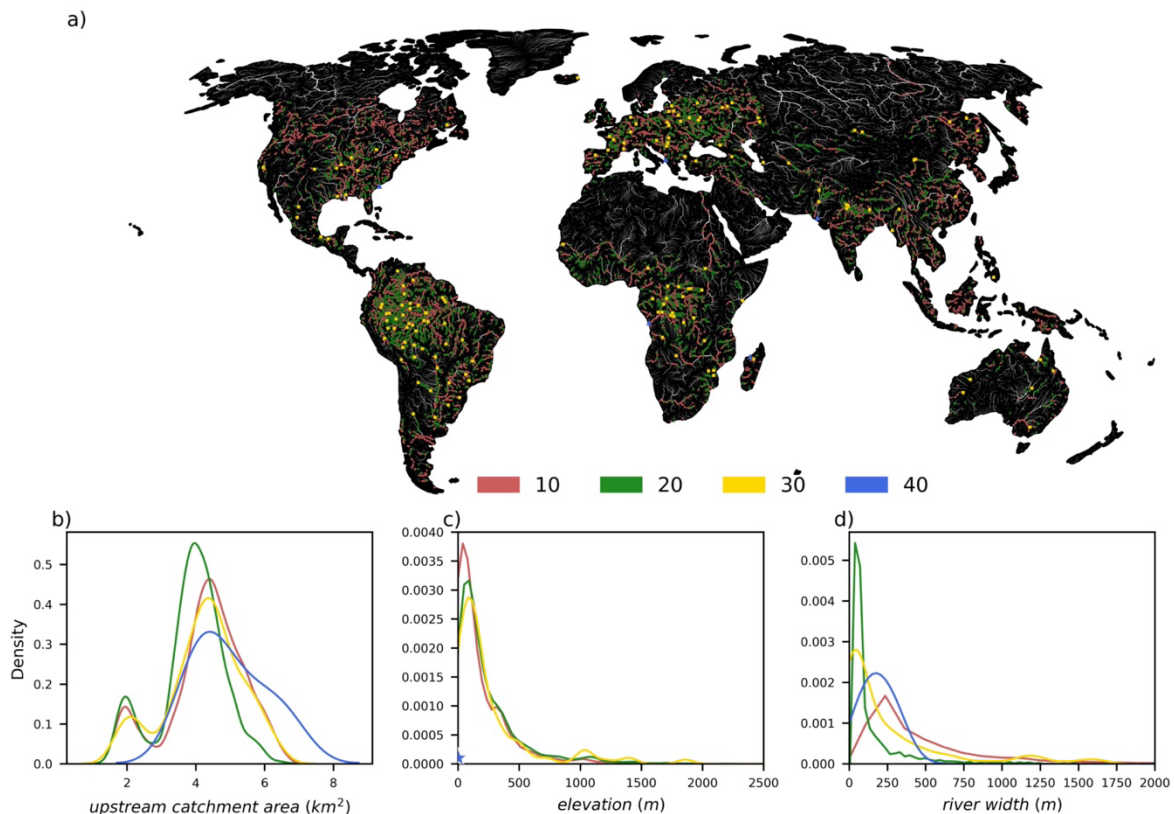


**Figure 4: Global map of allocation flags. Panel at lower left corner shows probability distribution of the upstream catchment area in log scale for different flags. Flags 10, 20, 30, and 40 are indicated by light blue, medium blue, dark blue, and red colors, respectively.**

275 20, and flag 30, respectively. Notably, flag 40 was not visible in Figure 4c due to its very low elevation, with a median of 0.0m (mean=0.54m and std=1.21m). Flags 10 to 30 were distributed from mean sea level to 4790.0m, and there was no significant difference in elevation observed among flags 10 to 30.

The river width distribution for each flag is demonstrated in Figure 4d. Flag 20 exhibited the smallest median river width at 41.4m, with a relatively low standard deviation of 193.3m. On the other hand, Flag 40 displayed the largest median river width of 224.0m, but its variation was substantial (std=1336.6m) due to the wider Congo downstream, which measures around 3170.0m. Flag 10 showed a median river width value of 222.0m, comparable to Flag 40, but with a lower variation (std=683.6m). Meanwhile, Flag 30 exhibited a median river width of 77.7m, falling between the median river widths of Flag 10 and Flag 40. The large variation in river width observed for Flag 10 was due to its widespread distribution across the rivers, while the substantial variation of Flag 40 was influenced by the VSs' location in the Congo River.

### 3.2 Biased VSs

Figure 5 shows the spatial heterogeneity of biased VSs, their distribution of upstream catchment areas in log scale, variation in their elevations, and a histogram of river widths at VS locations, calculated using MERIT Hydro. Biased VSs accounted for 2.6% of all VSs, and were distributed worldwide, with no distinct spatial pattern. A large number of them were allocated to large river basins such as the Amazon, Congo, and Mekong basins. Most

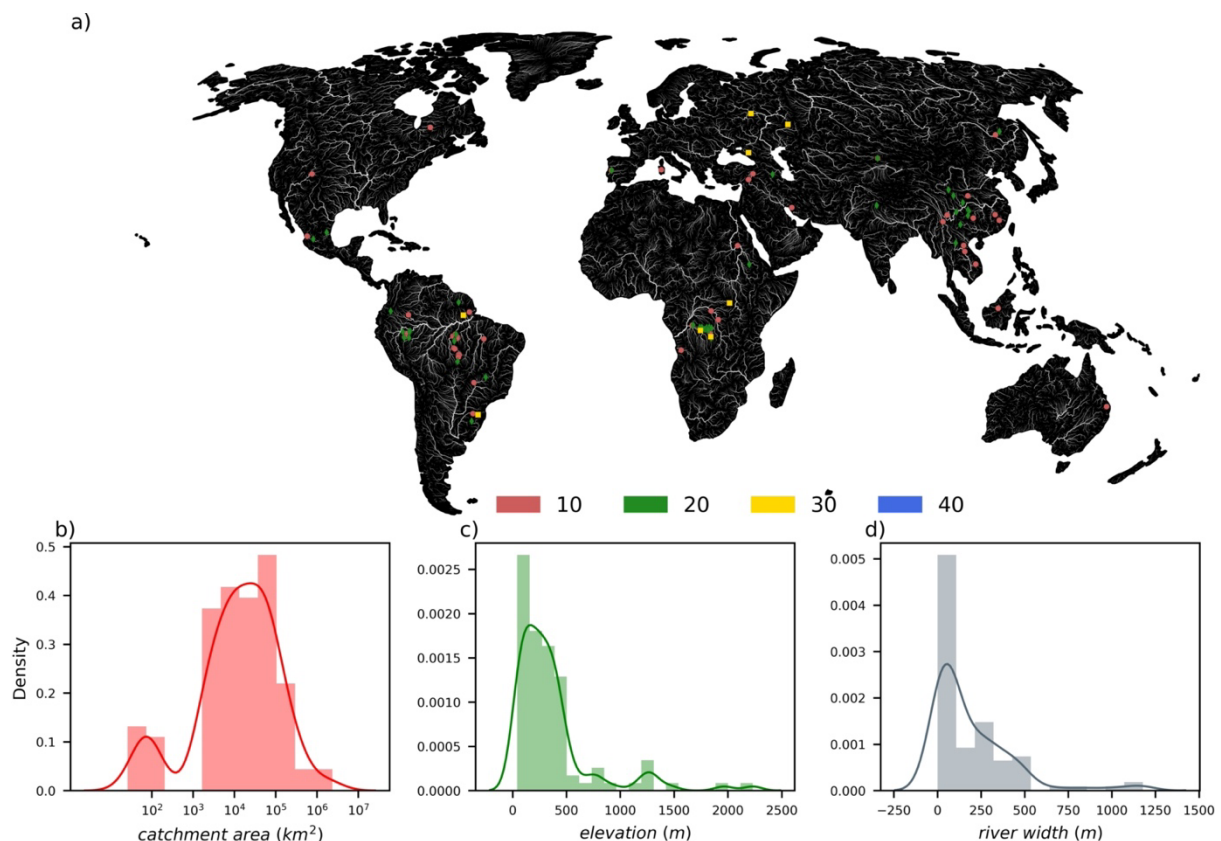


**Figure 5: a) Global distribution, b) histogram of catchment area (km<sup>2</sup>), c) histogram of elevation (m), and d) histogram of river width (m) of biased VSs. Light blue circles, medium blue diamonds, dark blue squares, and red triangles for flags 10, 20, 30, and 40, respectively in panel a.**

were flagged 20, which was the second most common allocation flag. Many were detected in the Amazon basin of South America. The median upstream catchment area of biased VSs was  $2.98 \times 10^4 \text{ km}^2$ , their median elevation was 199.6 m, and the median river width was 87.5 m, with most values ranging from 0 to 500 m. Thus, most biased VSs were detected in narrow rivers at high altitudes.

295 VSs with biased WSEs were generally found in narrow, high-elevation river reaches, although some were found in rivers such as the main Congo channel. Most biased VSs had WSEs that exceeded the MERIT Hydro feasible elevation range. Large biases can be caused by off-nadir measurement of nearby water bodies (Maillard et al., 2015), deviations of the MERIT Hydro river network from actual river (Amatulli et al., 2022), and DEM errors such as vegetation bias (Yamazaki et al., 2017). Further study is needed to fully understand the causes of errors  
300 in river WSEs obtained by satellite altimetry which is beyond the scope of this data description paper.

## 4 Discussion

### 4.1 Effect of discrete river reaches and DEM errors.

As the distance from the VS location to the unit catchment mouth increased, the median RMSE of simulated WSE increased (Figure 6), mainly due to the difference in elevation between these points. Thus, large errors may be  
305 associated with simulated WSE when the VS is located far from the unit catchment mouth. Similarly, the median RMSE of simulated WSE increased slightly as the slope within the unit-catchment increased until slope  $< 200 \text{ m/km}$ , with larger slopes ( $> 200 \text{ m/km}$ ) showing an increase in median RMSE from 2 to 4 m. This variation may have been caused by the non-uniformity of slopes within unit catchments of the CaMa-Flood model; however, it was well within the range of variation within unit-catchment slope bins, which reached up to 8 m.

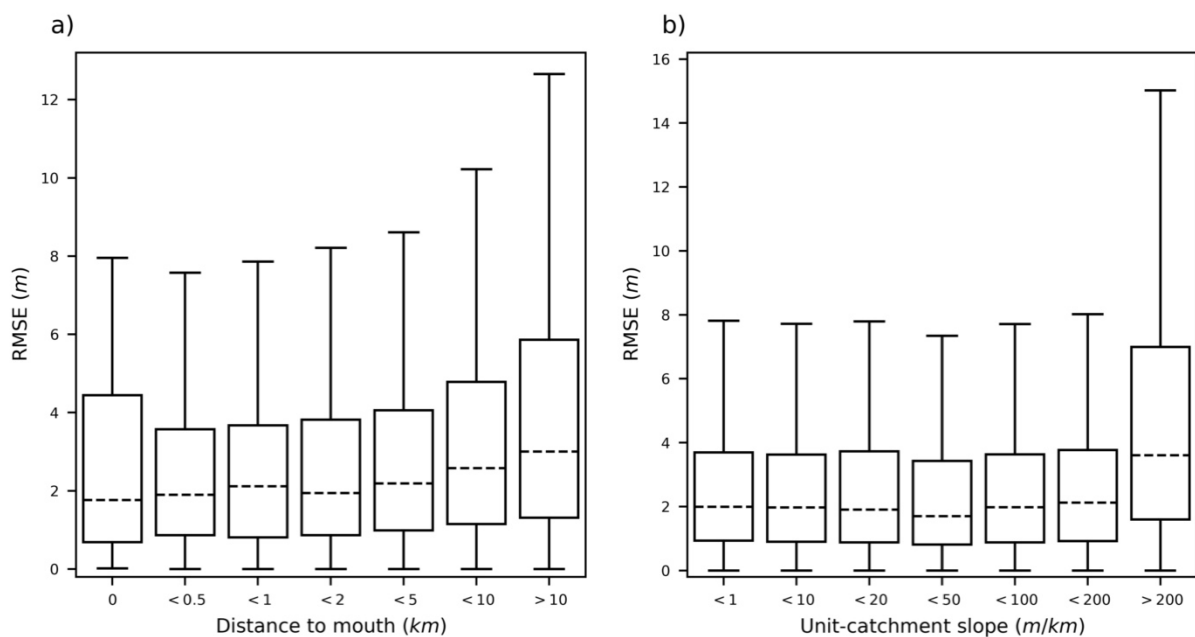


**Figure 6: Boxplot of the root mean square error (RMSE) against a) the distance to the unit-catchment mouth and b) unit-catchment slope.**

310 One of the main reasons for elevation bias between the satellite altimetry and model simulations is elevation  
differences between the VS locations and the base elevation of the model. This type of bias can be eliminated  
using the VS location as the unit-catchment mouth. However, this approach is challenging because unit-  
catchments size may be very small when several VSs located close to each other, which may lead to computational  
instability in CaMa-Flood model because it is optimized for unit-catchments of equal size. In addition, changing  
315 unit-catchment sizes can reduce the computational efficiency of the model drastically, which is critical for global-  
scale hydrodynamic models such as CaMa-Flood. Therefore, we did not consider updating the river network to  
use the VS locations as unit-catchment mouths in AltiMaP.

The allocation of VSs to a river network is highly dependent on the DEM used to delineate the river network  
(Schumann and Bates, 2018). Most freely available global-scale DEMs have large vertical errors that are  
320 accentuated over complex topography; these are unable to resolve microtopographic variation in relatively flat  
terrain (Chu and Lindenschmidt, 2017; Gallien et al., 2011). Although global-scale DEMs such as the Advanced  
Spaceborne Thermal Emission and Reflection Radiometer (ASTER) or Shuttle Radar Topography Mission  
(SRTM) exhibit non-negligible height errors, recent studies have attempted to eliminate these errors (e.g., Hawker  
et al., 2022; Rizzoli et al., 2017; Yamazaki et al., 2017). In this study, we used the MERIT DEM, which is a highly  
325 accurate global-scale DEM that is freely available (Hawker et al., 2019). Thus, AltiMaP can be applied to river  
networks delineated using any accurate global DEM.

#### 4.2 VS allocation to MERIT Hydro

Mapping the VSs to MERIT Hydro, a high-resolution global river network is a crucial step in leveraging their  
potential for hydrological modeling. There are several compelling reasons for mapping the VSs to MERIT Hydro,  
330 which is a high-resolution global river network at 3". Firstly, the mapping process can be easily adapted to various  
resolution river networks of the CaMa-Flood hydrodynamic model, such as 0.25° or 0.1°. This flexibility allows  
for the integration of VSs into a range of hydrological models, depending on the desired level of detail and  
accuracy. Secondly, the relative location of the VSs within the CaMa-Flood unit-catchment can be determined,

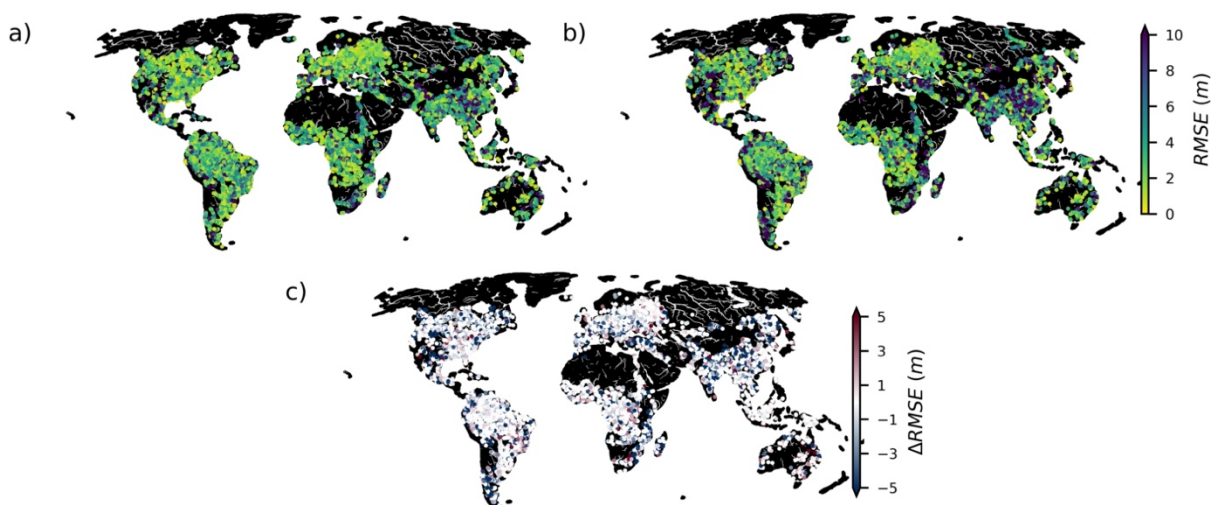


**Figure 7: Global map of root mean square error (*RMSE*) for a) AltiMaP and b) ordinary method; and c) *RMSE* difference ( $\Delta RMSE$ ) between expert and ordinary methods.**

which is essential for the calculation of important parameters such as elevation difference and distance to the unit  
335 catchment mouth (`dist_to_mouth`). These parameters are critical for evaluating and understanding the dynamics  
of water in a river network. Finally, the ability to allocate VS to any river network with a similar topology is  
demonstrated by mapping the VSs to MERIT Hydro, which is having D8 connectivity. Therefore, it is crucial to  
assign the VSs to the base map of the river network in the hydrodynamic model to enhance the evaluation of the  
models and to identify the causes for the discrepancies between the model and observations.

340 RMSEs were calculated for WSEs simulated by CaMa-Flood and forced by VIC BC runoff (Lin et al., 2019).  
Both simulations and observations were converted to the same geoid before calculating RMSE (i.e., EGM96).  
The spatial distributions of WSE RMSEs for VS allocations obtained using AltiMaP and the traditional method  
of allocating VSs to the CaMa-Flood grid are shown in Figure 7. Traditional VS allocation was performed using  
directly converting longitude and latitude information to coarse-resolution (i.e.,  $0.1^\circ$ ) grids. At the global scale,  
345 RMSEs were generally similar between both VS allocation methods. However, the satellite altimetry was better  
represented by AltiMaP for 17.52% of VSs (negative  $\Delta$ RMSE) and by the traditional method for only 12.85% of  
VSs (positive  $\Delta$ RMSE) The lower  $\Delta$ RMSE of ordinary method may be due to the fact allocation to a nearby grid  
by ordinary method compensate for the errors in the model such as river bathymetry error (Modi et al., 2022).

The AltiMaP and traditional VS allocation methods had median RMSEs of 7.86 and 8.70 m, respectively (Figure  
350 8). The inter-quartile range was larger for the traditional method. Thus, AltiMaP reduced the RMSE by 10.6%  
through more accurate VS allocation to the river network map. RMSE was reduced by AltiMaP for all flags, with  
the largest reduction observed in flag 30 (Table 3) due to VS allocation to more appropriate segments of multi-  
channel rivers, followed by flags 20, 10. But accuracy was slightly degraded in flag 40, in which VSs were  
allocated inward from the ocean. The remaining error may be attributed to elevation differences between VS  
355 locations and simulated WSE locations (Figure 3) and limitations of the hydrodynamic model.

A flag-wise comparison revealed that errors associated with the allocation method varied among flags in the  
AltiMaP results. Almost all AltiMaP flags had lower RMSE than those produced by the traditional method. This  
difference was due to the irregular shape of unit-catchments in the CaMa-Flood hydrodynamic model. In long,  
narrow unit catchments, slight deviations in VS location could lead to the misidentification of adjacent unit  
360 catchments as target grid. Thus, simulated WSEs deviated by 1–15 m, depending on the slope and river path (e.g.,

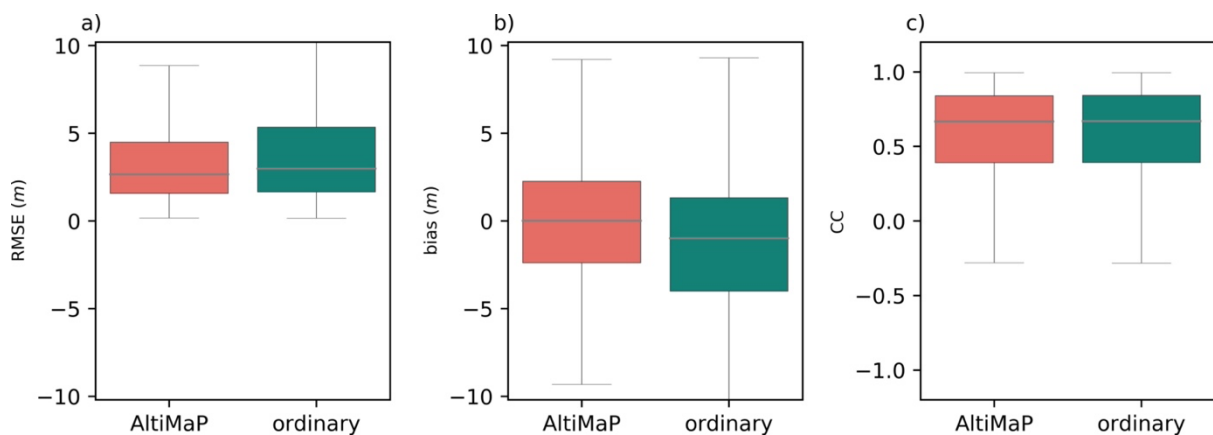


**Figure 8: Distribution of root mean square error (RMSE), bias, and correlation coefficient (CC) for AltiMaP and ordinary VS allocation methods in panels a, b, and d, respectively.**

straight vs. meandering river). These results highlight the importance of implementing specialized procedures such as AltiMaP to locate optimal river grid matches for each VS prior to WSE comparisons.

### 4.3 Advantage of mapping VSs

Because we used river network-related variables in the AltiMaP VS allocation algorithm, we were able to calculate distances and elevation differences between each VS and the unit-catchment river mouth. These parameters are particularly important for comparing WSEs simulated by coarse-resolution, large-scale river routing models such as CaMa-Flood, which are based on discretized river reaches with a representative elevation for each pixel. Minimizing the distance and elevation difference between the VS and unit-catchment river mouth is critical for improving the accuracy of WSE simulations. Thus, this elevation difference may be used as a proxy to interpret bias between simulated and observed WSEs (Fassoni-Andrade et al., 2021). Satellite altimetry data are also extremely useful for evaluating and calibrating hydrodynamic models (e.g., Zhou et al., 2022) and correcting variables through data assimilation (e.g., Revel et al., 2023b), which requires correct VS allocation to a river network map. The river bathymetry parameter can be calibrated using rating curve method developed using satellite altimetry and in-situ river discharge data (Zhou et al., 2022). Furthermore, the model can be evaluated using multi-variables (i.e., river discharge, WSE, and inundation extent) (Modi et al., 2022).

The flags used in AltiMaP to classify VSs provide a unique opportunity for users to identify the VS allocation methods used to evaluate hydrodynamic model outputs. Notably, simulated WSEs in first- and second-candidate river pixels for VSs that were initially allocated to multi-channel rivers (flag 30) can be used to select optimal VS locations along the river network. Most VSs flagged 10 were located in upstream reaches, whereas those flagged 30 and 40 were initially located in multi-channel rivers and oceans (which are most in need of relocation) and were allocated to downstream reaches. It is important to correctly allocate VSs initially located on multi-channel rivers because river networks based on the MERIT Hydro separate each channel of a multi-channel river into different unit-catchments. Thus, discrepancies in the allocation of VSs located on smaller channels can mistakenly alter the WSE dynamics of the simulation, such that the allocation flags are important indicators of VS usage in the context of hydrodynamic modeling.

**Table 3: Median statistics of the error of simulated WSE using CaMa-Flood hydrodynamic model. RMSE (root mean squared error), Bias, and CC (correlation coefficient) were presented. The simulated WSE is compared with HydroWeb satellite altimetry data where the VS s were allocated using AltiMaP or the ordinary allocation method.**

	AltiMaP			Ordinary		
	RMSE	bias	CC	RMSE	bias	CC
All	2.68	-0.01	0.67	2.98	-0.99	0.67
Flag 10	2.65	-0.43	0.67	2.94	-1.87	0.68
Flag 20	2.71	-0.17	0.66	3.06	-2.46	0.66
Flag 30	2.72	-0.60	0.64	2.85	-1.97	0.61
Flag 40	0.85	-0.37	0.02	0.94	-0.30	0.02



#### 390 4.4 Limitations and Future Perspectives

Even though AltiMaP is suitable in mapping the VSs into the given river network with D8 connection, the method is not capable of identifying non-nadir observations (such as floodplain lakes near the river channel). One of the major problem in the conventional altimeters in low-resolution mode (LRM) such as ENVISAT was correcting the observations from the non-nadir view was treated as nadir observations (Calmant et al., 2008; Frappart et al., 395 2006; da Silva et al., 2012). The dual antenna configuration of the CryoSat-2 allows precise position of reflecting point in the radar footprint and solve the signal location along-track and across-track directions (Cretaux, 2022). Moreover, ICESat-1/2 data can also be a great source of importance over terrestrial waters, but the longer revisit time limit the applications in hydrology. Satellites such as CryoSat-2 and ICESat-2 provide an addition challenge in using them in river monitoring. CryoSat-2 with its' drifting orbit ~7.5km makes it challenging to define VSs 400 as in repeat orbits (Schneider et al., 2017). With the complex ground track configuration of ICESat-2 makes it complex to use in river monitoring because the assigning method would differ depend on the satellite track orientation with respect to the river centerline (Scherer et al., 2023). However, with slight modification to the AltiMaP, we would be able to map such data into the MERIT Hydro (Supplementary Figure S2).

#### 5 Data availability

405 Data produced by AltiMaP were published in <https://doi.org/10.4211/hs.632e550deaca46b080bdae986fd19156> (Revel et al., 2022). MERIT Hydro river network data are freely available ([http://hydro.iis.u-tokyo.ac.jp/~yamada/MERIT\\_Hydro/](http://hydro.iis.u-tokyo.ac.jp/~yamada/MERIT_Hydro/)) under a Creative Commons license (CC-BY-NC 4.0).

#### 6 Code availability

The AltiMaP algorithm was published in <https://doi.org/10.5281/zenodo.7597310> (Revel et al., 2023a) and is 410 freely available for noncommercial use. The CaMa-Flood source codes are also available ([https://github.com/global-hydrodynamics/CaMa-Flood\\_v4](https://github.com/global-hydrodynamics/CaMa-Flood_v4)) under the Apache 2.0 license.

#### 7 Summary

We introduce AltiMaP, an effective methodology for comparing satellite altimetry WSE observations with WSEs simulated by large-scale hydrodynamic models such as CaMa-Flood. The procedure involves allocating each VS 415 to a suitable high-resolution (3") pixel, flagging the pixel according to land cover, and filtering out biased VSs according to the local MERIT DEM elevation. The main objective of this study was to improve the accuracy of allocation to a river network for a useful comparison of simulated and observed WSEs, among other applications. We compared WSEs simulated by the CaMa-Flood hydrodynamic model based on VIC BC runoff to satellite altimetry WSEs based on VS allocation to the MERIT Hydro river network using AltiMaP.

420 After mapping the flagged VSs to a 6' river network, biased VSs with values above or below the feasible MERIT Hydro elevation range were filtered out. Most VSs were located on single-channel rivers; VSs initially located on land were distributed worldwide. VSs initially located on multi-channel rivers and oceans were allocated to

downstream reaches of large rivers such as the Amazon, Congo, and Mekong Rivers. Biased VSs, incompatible with the river network elevation profile, were mainly found in narrow rivers at high elevations, likely because most altimeters are designed to observe ocean topography. Such VS biases are mainly caused by off-nadir measurements, DEM errors, or errors in the geolocation of river networks.

We also allocated VSs to a coarse-resolution CaMa-Flood river network for comparison with the simulated results. AltiMaP VS allocation represented the satellite altimetry more accurately than a traditional method, reducing the RMSE associated with the simulated WSEs by approximately 10%, representing a difference of approximately 2 m in multi-channel rivers. AltiMaP can be applied to any currently available processed satellite altimetry datasets (e.g., DAHITTI, Hydrosat, and CGLS) and any river network with simple land cover definitions (e.g., river, land, and ocean). We anticipate that the algorithm will contribute to the evaluation and/or calibration of hydrodynamic models using satellite altimetry and the acquisition of accurate hydrodynamic model output through satellite altimetry assimilation.

**8 Author contribution:** MR developed and finalized processing algorithms, performed the exploration of the methods, and finalized the manuscript. MR and DY designed the experiments. XZ and PM provided the data for comparison. JC and SC provided the expertise on deriving the satellite altimetry for rivers. All co-authors involved in revising and editing the manuscript.

**9 Competing interests:** The authors declare that they have no conflict of interest.

## 10 Acknowledgments

This work was supported by the Japan Society for the Promotion of Science (JSPS) under KIBAN-S Grant No.21H05002, JSPS KIBAN-B 20H02251, and JSPS start-up 20K22428. We extend our gratitude to the Topic editor James Thornton, four anonymous referees, and João Paulo Brêda for their valuable comments and suggestions.

## 11 References

Abdalla, S., Abdeh Kolahchi, A., Ablain, M., Adusumilli, S., Aich Bhowmick, S., Alou-Font, E., Amarouche, L., Andersen, O. B., Antich, H., Aouf, L., Arbic, B., Armitage, T., Arnault, S., Artana, C., Aulicino, G., Ayoub, N., Badulin, S., Baker, S., Banks, C., Bao, L., Barbetta, S., Barceló-Llull, B., Barlier, F., Basu, S., Bauer-Gottwein, P., Becker, M., Beckley, B., Bellefond, N., Belonenko, T., Benkiran, M., Benkouider, T., Bennartz, R., Benveniste, J., Bercher, N., Berge-Nguyen, M., Bettencourt, J., Blarel, F., Blazquez, A., Blumstein, D., Bonnefond, P., Borde, F., Bouffard, J., Boy, F., Boy, J. P., Brachet, C., Bresseur, P., Braun, A., Brocca, L., Brockley, D., Brodeau, L., Brown, S., Bruinsma, S., Bulczak, A., Buzzard, S., Cahill, M., Calmant, S., Calzas, M., Camici, S., Cancet, M., Capdeville, H., Carabjal, C. C., Carrere, L., Cazenave, A., Chassignet, E. P., Chauhan, P., Cherchali, S., Chereskin, T., Cheymol, C., Ciani, D., Cipollini, P., Cirillo, F., Cosme, E., Coss, S., Cotroneo, Y., Cotton, D., Couhert, A., Coutin-Faye, S., Crétaux, J. F., Cyr, F., d'Ovidio, F., Darrozes, J., David, C., Dayoub, N., De Staerke,

- D., Deng, X., Desai, S., Desjonqueres, J. D., Dettmering, D., Di Bella, A., Díaz-Barroso, L., Dibarboure, G., Dieng, H. B., Dinardo, S., Dobslaw, H., Dodet, G., Doglioli, A., Domeneghetti, A., Donahue, D., Dong, S., et al.: Altimetry for the future: Building on 25 years of progress, *Adv. Sp. Res.*, 68(2), 319–363, doi:10.1016/j.asr.2021.01.022, 2021.
- 460 Amatulli, G., Garcia Marquez, J., Sethi, T., Kiesel, J., Grigoropoulou, A., Üblacker, M. M., Shen, L. Q. and Domisch, S.: Hydrography90m: A new high-resolution global hydrographic dataset, *Earth Syst. Sci. Data*, 14(10), 4525–4550, doi:10.5194/essd-14-4525-2022, 2022.
- Asadzadeh Jarihani, A., Callow, J. N., Johansen, K. and Gouweleeuw, B.: Evaluation of multiple satellite altimetry data for studying inland water bodies and river floods, *J. Hydrol.*, 505, 78–90, doi:10.1016/j.jhydrol.2013.09.010, 2013.
- 465 Bates, P. D., Horritt, M. S. and Fewtrell, T. J.: A simple inertial formulation of the shallow water equations for efficient two-dimensional flood inundation modelling, *J. Hydrol.*, 387(1–2), 33–45, doi:10.1016/j.jhydrol.2010.03.027, 2010.
- Biancamaria, S., Frappart, F., Leleu, A. S., Marieu, V., Blumstein, D., Desjonquères, J. D., Boy, F., Sottolichio, A. and Valle-Levinson, A.: Satellite radar altimetry water elevations performance over a 200 m wide river: Evaluation over the Garonne River, *Adv. Sp. Res.*, 59(1), 128–146, doi:10.1016/j.asr.2016.10.008, 2017.
- 470 Birkett, C. M. and Beckley, B.: Investigating the Performance of the Jason-2/OSTM Radar Altimeter over Lakes and Reservoirs, *Mar. Geod.*, 33, 204–238, doi:10.1080/01490419.2010.488983, 2010.
- Birkett, C. M., Mertes, L. A. K., Dunne, T., Costa, M. H. and Jasinski, M. J.: Surface water dynamics in the Amazon Basin: Application of satellite radar altimetry, *J. Geophys. Res. Atmos.*, 107(20), LBA 26-1-LBA 26-21, doi:10.1029/2001JD000609, 2002.
- 475 Brêda, J. P. L. F., Paiva, R. C. D., Bravo, J. M., Passaia, O. A. and Moreira, D. M.: Assimilation of Satellite Altimetry Data for Effective River Bathymetry, *Water Resour. Res.*, 55(9), 7441–7463, doi:10.1029/2018WR024010, 2019.
- 480 Calmant, S. and Seyler, F.: Continental surface waters from satellite altimetry, *Comptes Rendus - Geosci.*, 338(14–15), 1113–1122, doi:10.1016/j.crte.2006.05.012, 2006.
- Calmant, S., Seyler, F. and Cretaux, J. F.: Monitoring continental surface waters by satellite altimetry, *Surv. Geophys.*, 29(4–5), 247–269, doi:10.1007/s10712-008-9051-1, 2008.
- Calmant, S., Da Silva, J. S., Moreira, D. M., Seyler, F., Shum, C. K., Crétaux, J. F. and Gabalda, G.: Detection of Envisat RA2/ICE-1 retracked radar altimetry bias over the Amazon basin rivers using GPS, *Adv. Sp. Res.*, 51(8), 1551–1564, doi:10.1016/j.asr.2012.07.033, 2013.
- 485 Chu, T. and Lindenschmidt, K. E.: Comparison and Validation of Digital Elevation Models Derived from InSAR for a Flat Inland Delta in the High Latitudes of Northern Canada, *Can. J. Remote Sens.*, 43(2), 109–123, doi:10.1080/07038992.2017.1286936, 2017.
- 490 Coss, S., Durand, M., Yi, Y., Jia, Y., Guo, Q., Tuozzolo, S., Shum, C. K., Allen, G. H., Calmant, S. and Pavelsky,

- T.: Global River Radar Altimetry Time Series (GRRATS): New river elevation earth science data records for the hydrologic community, *Earth Syst. Sci. Data*, 12(1), 137–150, doi:10.5194/essd-12-137-2020, 2020.
- Crétaux, J.-F.: *Inland Water Altimetry: Technological Progress and Applications*, edited by F. Di Mauro, A., Scozzari, A., Soldovieri, pp. 111–139, Springer Water. Springer, Cham., 2022.
- 495 Crétaux, J. F., Calmant, S., Romanovski, V., Shabunin, A., Lyard, F., Bergé-Nguyen, M., Cazenave, A., Hernandez, F. and Perosanz, F.: An absolute calibration site for radar altimeters in the continental domain: Lake Issykkul in Central Asia, *J. Geod.*, 83(8), 723–735, doi:10.1007/s00190-008-0289-7, 2009.
- Crétaux, J. F., Arsen, A., Calmant, S., Kouraev, A., Vuglinski, V., Bergé-Nguyen, M., Gennero, M. C., Nino, F., Abarca Del Rio, R., Cazenave, A. and Maisongrande, P.: SOLS: A lake database to monitor in the Near Real  
500 Time water level and storage variations from remote sensing data, *Adv. Sp. Res.*, 47(9), 1497–1507, doi:10.1016/j.asr.2011.01.004, 2011.
- Dettmering, D., Ellenbeck, L., Scherer, D., Schwatke, C. and Niemann, C.: Potential and limitations of satellite altimetry constellations for monitoring surface water storage changes—A case study in the Mississippi basin, *Remote Sens.*, 12(20), 1–19, doi:10.3390/rs12203320, 2020.
- 505 Domeneghetti, A., Molari, G., Tourian, M. J., Tarpanelli, A., Behnia, S., Moramarco, T., Sneeuw, N. and Brath, A.: Testing the use of single- and multi-mission satellite altimetry for the calibration of hydraulic models, *Adv. Water Resour.*, 103887, doi:10.1016/j.advwatres.2021.103887, 2021.
- Elmer, N. J., McCreight, J. and Hain, C.: Hydrologic Model Parameter Estimation in Ungauged Basins Using Simulated SWOT Discharge Observations, *Water Resour. Res.*, 57(10), 1–18, doi:10.1029/2021WR029655, 2021.
- 510 Fassoni-Andrade, A. C., Fleischmann, A. S., Papa, F., Paiva, R. C. D. de, Wongchuig, S., Melack, J. M., Moreira, A. A., Paris, A., Ruhoff, A., Barbosa, C., Maciel, D. A., Novo, E., Durand, F., Frappart, F., Aires, F., Abrahão, G. M., Ferreira-Ferreira, J., Espinoza, J. C., Laipelt, L., Costa, M. H., Espinoza-Villar, R., Calmant, S. and Pellet, V.: Amazon Hydrology From Space: Scientific Advances and Future Challenges, *Rev. Geophys.*, 59(4), 1–97, doi:10.1029/2020RG000728, 2021.
- 515 Frappart, F., Calmant, S., Cauhopé, M., Seyler, F. and Cazenave, A.: Preliminary results of ENVISAT RA-2-derived water levels validation over the Amazon basin, *Remote Sens. Environ.*, 100(2), 252–264, doi:10.1016/j.rse.2005.10.027, 2006.
- Gallien, T. W., Schubert, J. E. and Sanders, B. F.: Predicting tidal flooding of urbanized embayments: A modeling framework and data requirements, *Coast. Eng.*, 58(6), 567–577, doi:10.1016/j.coastaleng.2011.01.011, 2011.
- 520 Hannah, D. M., Demuth, S., van Lanen, H. A. J., Looser, U., Prudhomme, C., Rees, G., Stahl, K. and Tallaksen, L. M.: Large-scale river flow archives: Importance, current status and future needs, *Hydrol. Process.*, 25(7), 1191–1200, doi:10.1002/hyp.7794, 2011.
- Hawker, L., Neal, J. and Bates, P.: Accuracy assessment of the TanDEM-X 90 Digital Elevation Model for selected floodplain sites, *Remote Sens. Environ.*, 232(July), doi:10.1016/j.rse.2019.111319, 2019.
- 525 Hawker, L., Uhe, P., Paulo, L., Sosa, J., Savage, J., Sampson, C. and Neal, J.: A 30 m global map of elevation

with forests and buildings removed, *Environ. Res. Lett.*, 17(2), doi:10.1088/1748-9326/ac4d4f, 2022.

Jiang, L., Madsen, H. and Bauer-Gottwein, P.: Simultaneous calibration of multiple hydrodynamic model parameters using satellite altimetry observations of water surface elevation in the Songhua River, *Remote Sens. Environ.*, 225(March), 229–247, doi:10.1016/j.rse.2019.03.014, 2019.

530 Jiang, L., Westphal Christensen, S. and Bauer-Gottwein, P.: Calibrating 1D hydrodynamic river models in the absence of cross-section geometry using satellite observations of water surface elevation and river width, *Hydrol. Earth Syst. Sci.*, 25(12), 6359–6379, doi:10.5194/hess-25-6359-2021, 2021a.

Jiang, L., Christensen, S. W. and Bauer-Gottwein, P.: Calibrating 1D hydrodynamic river models in the absence of cross-sectional geometry: A new parameterization scheme, *Hydrol. Earth Syst. Sci. Discuss.*, (April), 1–14, 535 doi:10.5194/hess-2021-210, 2021b.

Kittel, C. M. M., Hatchard, S., Neal, J. C., Nielsen, K., Bates, P. D. and Bauer-Gottwein, P.: Hydraulic Model Calibration Using CryoSat-2 Observations in the Zambezi Catchment, *Water Resour. Res.*, 57(9), 1–19, doi:10.1029/2020WR029261, 2021.

Liang, X., Lettenmaier, D. P., Wood, E. F. and Burges, S. J.: A simple hydrologically based model of land surface 540 water and energy fluxes for general circulation models, *J. Geophys. Res.*, 99(D7), 14415, doi:10.1029/94JD00483, 1994.

Lin, P., Pan, M., Beck, H. E., Yang, Y., Yamazaki, D., Frasson, R., David, C. H., Durand, M., Pavelsky, T. M., Allen, G. H., Gleason, C. J. and Wood, E. F.: Global Reconstruction of Naturalized River Flows at 2.94 Million Reaches, *Water Resour. Res.*, 55(8), 6499–6516, doi:10.1029/2019WR025287, 2019.

545 Maillard, P., Bercher, N. and Calmant, S.: New processing approaches on the retrieval of water levels in Envisat and SARAL radar altimetry over rivers: A case study of the São Francisco River, Brazil, *Remote Sens. Environ.*, 156, 226–241, doi:10.1016/j.rse.2014.09.027, 2015.

Meyer Oliveira, A., Fleischmann, A. S. and Paiva, R. C. D.: On the contribution of remote sensing-based calibration to model hydrological and hydraulic processes in tropical regions, *J. Hydrol.*, 597, 126184, 550 doi:10.1016/j.jhydrol.2021.126184, 2021.

Michailovsky, C. I., Milzow, C. and Bauer-Gottwein, P.: Assimilation of radar altimetry to a routing model of the Brahmaputra River, *Water Resour. Res.*, 49(8), 4807–4816, doi:10.1002/wrcr.20345, 2013.

Modi, P., Revel, M. and Yamazaki, D.: Multivariable Integrated Evaluation of Hydrodynamic Modeling: A Comparison of Performance Considering Different Baseline Topography Data, *Water Resour. Res.*, 58(8), 1–20, 555 doi:10.1029/2021WR031819, 2022.

Paiva, R. C. D., Collischonn, W., Bonnet, M. P., De Gonçalves, L. G. G., Calmant, S., Getirana, A. and Santos Da Silva, J.: Assimilating in situ and radar altimetry data into a large-scale hydrologic-hydrodynamic model for streamflow forecast in the Amazon, *Hydrol. Earth Syst. Sci.*, 17(7), 2929–2946, doi:10.5194/hess-17-2929-2013, 2013.

560 De Paiva, R. C. D., Buarque, D. C., Collischonn, W., Bonnet, M. P., Frappart, F., Calmant, S. and Bulhões Mendes,

- C. A.: Large-scale hydrologic and hydrodynamic modeling of the Amazon River basin, *Water Resour. Res.*, 49(3), 1226–1243, doi:10.1002/wrcr.20067, 2013.
- Papa, F., Crétaux, J.-F., Grippa, M., Robert, E., Trigg, M., Tshimanga, R. M., Kitambo, B., Paris, A., Carr, A., Fleischmann, A. S., de Fleury, M., Gbetkom, P. G., Calmettes, B. and Calmant, S.: Water Resources in Africa under Global Change: Monitoring Surface Waters from Space., 2022.
- Paz, A. R., Collischonn, W. and Lopes Da Silveira, A. L.: Improvements in large-scale drainage networks derived from digital elevation models, *Water Resour. Res.*, 42(8), 1–7, doi:10.1029/2005WR004544, 2006.
- Pekel, J. F., Cottam, A., Gorelick, N. and Belward, A. S.: High-resolution mapping of global surface water and its long-term changes, *Nature*, 540(7633), 418–422, doi:10.1038/nature20584, 2016.
- 570 Revel, M., Zhou, X., Modi, P., Yamazaki, D., Calmant, S. and Cretaux, J.-F.: AltiMaP v1.0, , doi:https://doi.org/10.4211/hs.632e550deaea46b080bdae986fd19156, 2022.
- Revel, M., Zhou, X., Modi, P., Yamazaki, D., Calmant, S. and Cretaux., J.-F.: AltiMaP v1.0, , doi:https://doi.org/10.5281/zenodo.7597310, 2023a.
- Revel, M., Zhou, X., Yamazaki, D. and Kanae, S.: Assimilation of transformed water surface elevation to improve river discharge estimation in a continental-scale river, *Hydrol. Earth Syst. Sci.*, 27(3), 647–671, doi:10.5194/hess-27-647-2023, 2023b.
- 575 Rizzoli, P., Martone, M., Gonzalez, C., Wecklich, C., Borla Tridon, D., Bräutigam, B., Bachmann, M., Schulze, D., Fritz, T., Huber, M., Wessel, B., Krieger, G., Zink, M. and Moreira, A.: Generation and performance assessment of the global TanDEM-X digital elevation model, *ISPRS J. Photogramm. Remote Sens.*, 132, 119–139, doi:10.1016/j.isprsjprs.2017.08.008, 2017.
- 580 Santos da Silva, J., Calmant, S., Seyler, F., Rotunno Filho, O. C., Cochonneau, G. and Mansur, W. J.: Water levels in the Amazon basin derived from the ERS 2 and ENVISAT radar altimetry missions, *Remote Sens. Environ.*, 114(10), 2160–2181, doi:10.1016/j.rse.2010.04.020, 2010.
- Scherer, D., Schwatke, C., Dettmering, D. and Seitz, F.: ICESat-2 river surface slope (IRIS): A global reach-scale water surface slope dataset, *Sci. Data*, 10(1), 1–13, doi:10.1038/s41597-023-02215-x, 2023.
- 585 Schneider, R., Nygaard Godiksen, P., Villadsen, H., Madsen, H. and Bauer-Gottwein, P.: Application of CryoSat-2 altimetry data for river analysis and modelling, *Hydrol. Earth Syst. Sci.*, 21(2), 751–764, doi:10.5194/hess-21-751-2017, 2017.
- Schumann, G. J. P. and Bates, P. D.: The Need for a High-Accuracy, Open-Access Global DEM, *Front. Earth Sci.*, 6(December), 1–5, doi:10.3389/feart.2018.00225, 2018.
- 590 Schwatke, C., Dettmering, D., Bosch, W. and Seitz, F.: DAHITI - An innovative approach for estimating water level time series over inland waters using multi-mission satellite altimetry, *Hydrol. Earth Syst. Sci.*, 19(10), 4345–4364, doi:10.5194/hess-19-4345-2015, 2015.
- da Silva, J. S., Seyler, F., Calmant, S., Filho, O. C. R., Roux, E., Araújo, A. A. M. and Guyot, J. L.: Water level dynamics of Amazon wetlands at the watershed scale by satellite altimetry, *Int. J. Remote Sens.*, 33(11), 3323–
- 595

3353, doi:10.1080/01431161.2010.531914, 2012.

Tourian, M. J., Tarpanelli, A., Elmi, O., Qin, T., Brocca, L., Moramarco, T. and Sneeuw, N.: Spatiotemporal densification of river water level time series by multimission satellite altimetry, *Water Resour. Res.*, 52(2), 1140–1159, doi:10.1002/2015WR017654, 2016.

600 Tourian, M. J., Elmi, O., Shafaghi, Y., Behnia, S. and Saemian, P.: HydroSat : geometric quantities of the global water cycle from geodetic satellites, , 2463–2486, 2022.

Trigg, M. A., Wilson, M. D., Bates, P. D., Horritt, M. S., Alsdorf, D. E., Forsberg, B. R. and Vega, M. C.: Amazon flood wave hydraulics, *J. Hydrol.*, 374(1–2), 92–105, doi:10.1016/j.jhydrol.2009.06.004, 2009.

Xiang, J., Li, H., Zhao, J., Cai, X. and Li, P.: Inland water level measurement from spaceborne laser altimetry: 605 Validation and comparison of three missions over the Great Lakes and lower Mississippi River, *J. Hydrol.*, 597(68), 126312, doi:10.1016/j.jhydrol.2021.126312, 2021.

Yamazaki, D., Oki, T. and Kanae, S.: Deriving a global river network map and its sub-grid topographic characteristics from a fine-resolution flow direction map, *Hydrol. Earth Syst. Sci.*, 13(11), 2241–2251, doi:10.5194/hess-13-2241-2009, 2009.

610 Yamazaki, D., Kanae, S., Kim, H. and Oki, T.: A physically based description of floodplain inundation dynamics in a global river routing model, *Water Resour. Res.*, 47(4), 1–21, doi:10.1029/2010WR009726, 2011.

Yamazaki, D., Lee, H., Alsdorf, D. E., Dutra, E., Kim, H., Kanae, S. and Oki, T.: Analysis of the water level dynamics simulated by a global river model: A case study in the Amazon River, *Water Resour. Res.*, 48(9), 1–15, doi:10.1029/2012WR011869, 2012.

615 Yamazaki, D., O’Loughlin, F., Trigg, M. A., Miller, Z. F., Pavelsky, T. M. and Bates, P. D.: Development of the Global Width Database for Large Rivers, *Water Resour. Res.*, 50(4), 3467–3480, doi:10.1002/2013WR014664, 2014a.

Yamazaki, D., Sato, T., Kanae, S., Hirabayashi, Y. and Bates, P. D.: Regional flood dynamics in a bifurcating mega delta simulated in a global river model, *Geophys. Res. Lett.*, 41(9), 3127–3135, doi:10.1002/2014GL059744, 620 2014b.

Yamazaki, D., Trigg, M. A. and Ikeshima, D.: Development of a global ~90m water body map using multi-temporal Landsat images, *Remote Sens. Environ.*, 171, 337–351, doi:10.1016/j.rse.2015.10.014, 2015.

Yamazaki, D., Ikeshima, D., Tawatari, R., Yamaguchi, T., O’Loughlin, F., Neal, J. C., Sampson, C. C., Kanae, S. and Bates, P. D.: A high-accuracy map of global terrain elevations, *Geophys. Res. Lett.*, 44(11), 5844–5853, 625 doi:10.1002/2017GL072874, 2017.

Yamazaki, D., Ikeshima, D., Sosa, J., Bates, P. D., Allen, G. H. and Pavelsky, T. M.: MERIT Hydro: A High-Resolution Global Hydrography Map Based on Latest Topography Dataset, *Water Resour. Res.*, 55(6), 5053–5073, doi:10.1029/2019WR024873, 2019.

Yang, L., Lin, L., Fan, L., Liu, N., Huang, L., Xu, Y., Mertikas, S. P., Jia, Y. and Lin, M.: Satellite Altimetry : 630 Achievements and Future Trends by a Scientometrics Analysis, , 1–22, 2022.

Zhou, X., Revel, M., Modi, P., Shiozawa, T. and Yamazaki, D.: Correction of River Bathymetry Parameters Using the Stage–Discharge Rating Curve, *Water Resour. Res.*, 58(4), 1–26, doi:10.1029/2021WR031226, 2022.